Proceedings of the Combustion Institute, Volume 36, Issue 2, 2017, Pages 1937–1945

A PDF approach to thin premixed flamelets using multiple mapping conditioning

B. Sundaram, A.Y. Klimenko

The University of Queensland, School of Mechanical and Mining Engineering, QLD 4072, Australia

Abstract

This work discusses the principles and application of the multiple mapping conditioning (MMC) framework to the simulation of turbulent premixed combustion. While it is clear that, conceptually, MMC allows for the enforcement of the consistency of probability density function (PDF) models with the flamelet limit, the implementation of this idea is non-trivial and requires substantial analysis. This work focuses on the principles of selecting reference variables suitable for the simulation of general premixed combustion cases. Reference variables based on the level set, shadow positions and progress variable are considered. The concept of second conditioning introduces a hierarchy of MMC models to combine both generality and computational efficiency. The paper presents stochastic simulations to demonstrate these principles.

Keywords: multiple mapping conditioning, probability density function, flamelet regime, turbulent premixed combustion

1. Introduction

The non-linear, multi-scale interactions between turbulent fluctuations and chemistry have been discussed [1, 2, 3, 4, 5, 6], and numerous approaches to the problem have been suggested. Modeling approaches can be categorized as those either based exclusively on, or a combination of: i) mixture fraction or progress variable methods such as fast chemistry [7], flamelet [3] and conditional moment closure (CMC) [8]; or ii) joint probability density function (PDF) [9, 10] methods which aim to reproduce the stochastic properties of reactive species. The generality and computational expense of the latter category exceeds that of the former. The attraction of PDF methods lies in their closure of chemical source terms, and their flexibility in simulating various regimes of combustion. In addition to computational cost, a non-trivial aspect of PDF methods is the introduction of an unclosed conditional scalar dissipation term modeled via a mixing operation. Both mixture fraction-based and PDF categories can be used in the context of Reynolds-averaged Navier-Stokes (RANS) methods or large eddy simulations (LES). The application of a third category called direct numerical simulation (DNS) for realistic cases, currently remains beyond modern computers due to extreme computational costs.

While the flamelet-based and PDF categories were conventionally viewed as distinct and incompatible, recent research is marked by the emergence of more universal approaches, which are currently represented by the multiple mapping conditioning (MMC) framework [11, 12] which combine the useful features of each category. While the application of MMC models to non-premixed flames has been demonstrated [13, 14], the question of finding an efficient framework for premixed flames remains open. Pope [15] notes that the Euclidean Minimum Spanning Tree (EMST) mixing model is consistent with the flamelet limit for non-premixed cases. (The presence of the mixture fraction PDF in the flamelet model is due to the linear approximation of the edge coefficients in EMST. A more accurate approximation of these coefficients should make EMST fully consistent with the standard non-premixed flamelet equation, but this property does not extend to premixed flames.) The conventional PDF method works reasonably for distributed premixed flames, but the application of non-local mixing models to premixed flamesheets is questionable as it results in the direct mixing of fluids across the flame front. Incorporating flamelet structures into PDF simulations has been discussed [16, 17, 18, 19, 20, 21].

MMC is advantageous as it can accommodate flamesheet regimes, and indeed distributed and intermediate regimes, into PDF simulations without compromising chemical source terms and the mixing operation. While MMC offers flexible flamelet-like control as part of PDF modeling, the remaining problem of premixed

Email address: brruntha.sundaram@uqconnect.edu.au (B. Sundaram)

combustion is a lack of understanding of the behavior of turbulent premixed flames; despite a large volume of results, reliable approximations for turbulent propagation speeds and parameter scalings through the inertial interval do not exist, inevitably limiting the extent and performance of models. In non-premixed flames, MMC has more accurate control of conditional fluctuations and, like CMC, MMC involving mixture fraction conditioning is flamelet-consistent and has the property of being consistent with the law of the inertial interval [22]. For premixed flame modeling, the first property is instrumental, and while the second can be preserved by proper conditioning, the third property is likely to be lost, as discussed later.

This work introduces a general MMC framework for premixed combustion focusing on possible selections of the reference variables. Unlike the previous work [23] dealing with a specific geometry and reference variable, general issues are discussed. The advantages and disadvantages of the MMC models, and basic demonstrative simulations are presented.

2. MMC concepts for modeling premixed combustion

MMC was first introduced [11] as an amalgamation of the PDF method [9], CMC [8] and mapping closure [24, 25]. It is the conditioning of the mixing operation on a set of reference variables, which are related to the physical quantities in turbulent combustion. Conditioning on reference variables, which is characterized by a localness parameter that determines the degree of mixing localization, is a feature common to all MMC models. Original MMC was extended to a generalized MMC framework for greater flexibility in the selection of reference variables, which can be represented by any useful physical quantities that are independent from, yet correlated to, key quantities of the specific case. Conditioning of the mixing operation affects, but does not compromise, the emulation of mixing. We assume unity Lewis and Schmidt numbers as well as constant density here, noting that MMC can be formulated for non-unity cases [26] and non-constant density [14]. Equations representing generic MMC models for velocity-scalar modeling (for both non-premixed and premixed cases) can be written as

$$d\mathbf{v}^* = \frac{\mathbf{V}^* - \mathbf{v}^*}{\tau_t} dt + (2\mathcal{B})^{1/2} d\omega^*_{\mathbf{u}}, \tag{1}$$

$$d\mathbf{x}^* = \mathbf{v}^* dt, \tag{2}$$

$$d\xi^*_i = a_i(\xi^*)dt + b_i(\xi^*)d\omega^*_\xi, \tag{3}$$

$$dY^*_I = (W_I(\mathbf{Y}^*) + \mathbb{S}[Y^*_I])dt \tag{4}$$

$$\langle \mathbb{S}_I[Y^*_I] \ |\mathbf{x}, \xi_1, ..., \xi_k\rangle = 0 \tag{5}$$

Here, the asterisk indicates that a quantity is stochastic while independent Wiener processes are denoted by ω^*. Equations (1)-(4) for $\mathbf{v}$, $\mathbf{x}$, ξ and Y model the physical velocity, position, reference variable and reactive scalar of a particle respectively. In Eq. (1), $\mathbf{V}$ is the mean velocity, τ_t is the the macro timescale while $\mathcal{B}$ controls the velocity rms and is related to the turbulent dissipation as $\mathcal{B} \sim \langle\varepsilon\rangle$ [27]. Equation (3) for the reference variable contains drift a_i and diffusion coefficients $D_i = b_i^2/2$. Equation (4) specifies the evolution of chemical species Y_I, $I = 1, 2, ..., n_s$ due to chemical reactions W_I and a mixing operation $\mathbb{S}$. Mixing is unrestricted to specific models, although Curl's [28], modified Curl's [29] and the interaction by exchange with the mean (IEM) [30] are common selections. The reference variables affect reactive scalars only through the localization of mixing as specified by (5). In generalized MMC [31], the set $\xi_1, ..., \xi_k$ may represent an arbitrary subset of all reference variables. In original MMC, conditioning must be performed on all reference variables.

For premixed combustion in the flamelet regime, non-local mixing models do not distinguish fresh reactants from burned products, allowing direct mixing of the fluid parcels from both these regions. The effect of MMC on premixed flame behavior is the prevention of this direct mixing between burned and unburned fluids. Physically, mixing occurs in a multi-stage process that gradually increases the mixture's temperature to the point of igniting. Hence, the MMC reference variable should distinguish a burned and unburned fluid parcel to prevent unphysical mixing and resolve the internal structure of the flame while reproducing the mixing and diffusion that occurs within the flamelet.

While the physical basis of MMC treatment of premixed combustion is seemingly transparent to the point of self-evidence, selection of suitable reference variables is far from simple. Generally, reference variables are used for conditioning, so only the topological structure of these variables matters. For example, conditioning on reference variable ξ and conditioning on $\xi' = f(\xi)$ where f is strictly monotonic, are conceptually equivalent. Practically, the choice of reference variables is important as an inappropriate selection may produce unstable, inaccurate or inefficient simulations. The selection of premixed reference variables is now discussed.

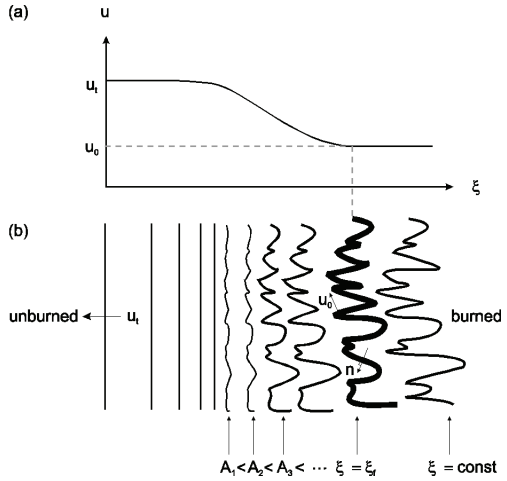

Figure 1: A schematic of the level set reference variable for a turbulent premixed flame; a) the reduction of drift velocity from the turbulent propagation speed u_t to the laminar flame speed u_0 in ξ-space as the flame front $\xi = \xi_f$ is approached and b) the increase in the area A_ξ of the ξ isosurfaces close to the flame front.

3. Level set reference variables

The rationale given in the previous section indicates that selecting a distance from the flame (i.e. closest distance to the reaction zone) is a natural choice for the reference variable in premixed combustion, producing the most transparent physical interpretation for MMC conditioning. This type of reference variable has proven effective when used in conditional models simulating reacting flows in porous media (e.g. the porous distance-based CMC model (PDCMC) [32]). The distance from the flame is conventionally referred to as the level set variable [3]. This variable ξ has a unit gradient $|\nabla\xi| = 1$ at regular points, although the field $\xi(\mathbf{x}, t)$ has many singularities where gradients are undefined. The level set approach has been deployed in various premixed models [33] as well as for effective asymptotic analysis of premixed flames disturbed by fluid flow [34].

Let $\xi \ll \xi_f$ in the unburned fluid and $\xi \gg \xi_f$ in the burned fluid as shown in Fig. 1, a conceptual consideration of the flame front, where the subscript f represents the flame location. As the flow characteristics depend more strongly on ξ than on the physical location x, we interpret ξ as an independent variable and average over x in the following consideration. In the ξ-space, the drift velocity $u(\xi)$ reduces from the turbulent propagation speed $u = u_t$ as $\xi \to -\infty$ to the laminar speed $u = u_0$ as $\xi \to \xi_f$. The overall mass flux must remain constant $u(\xi)P_\xi\rho_\xi = \text{const}$ where $\rho_\xi = \langle\rho|\xi\rangle$. P_ξ is the PDF of the scalar ξ which is proportional $P_\xi \sim A_\xi$ to the area A_ξ of the surfaces $\xi = \text{const}$ (per volume) due to the Bilger relation of $A_\xi \sim |\nabla\xi|\, P_\xi$ with the unit gradient $|\nabla\xi| = 1$ in Ref. [35]. We recall that in stochastic simulations, the particle-assigned values of ξ^* evolve according to a general Markov model that is specified by the Ito equation,

$$d\xi^* = u(\xi)dt + \big(2D(\xi)\big)^{1/2} d{\omega_\xi}^*, \tag{6}$$

where the coefficients $u(\xi)$ and $D(\xi)$ represent the propagation speed and the diffusion coefficient in ξ-space. These coefficients are in fact functions of $d = |\xi^* - \xi_f|$, which is interpreted as the distance from the flame. We do not yet consider physical locations x, which would need an additional relaxation term in Eq.(6) that localizes the surface $\xi = \xi_f$ in physical space (as is done in the shadow position mixing model (SPMM) [36]).

The parameters, $u(\xi)$ and $D(\xi)$ are determined by the scaling of the flame characteristics through the inertial interval. This scaling is linked to the cascade interpretation for premixed flame propagation [37]. The flame position is filtered with a characteristic scale d and, for each d, the it propagates with a given speed $u(d)$ due to effective diffusion $D(d)$ and reaction rates. If $d \to 0$, the flame characteristics are those of a laminar flame and $u(0) = u_0$. If $d \to \infty$, then $u(d) = u_t$, the turbulent propagation speed of the flame. The surface $\xi = \xi^1$, located at the distance $d = |\xi_f - \xi^1|$ from the flame, is the effective position of the flame which is not only shifted by d but also averaged over all variations of locations smaller than d (i.e. a d-scale filtering; both the surfaces of $\xi = \xi_f$ and $\xi = \xi^1$ have the same large-scale structure at scales greater than d). The scaling of flame characteristics through this inertial interval remain essentially unknown — only the limiting values of $u = u_0$ and $u = u_t$ have been extensively investigated. While Appendix I follows the cascade hypothesis [37] and presents a possible scaling, there is a large degree of uncertainty and lack of experimental data for behaviour of turbulent premixed flames at different scales.

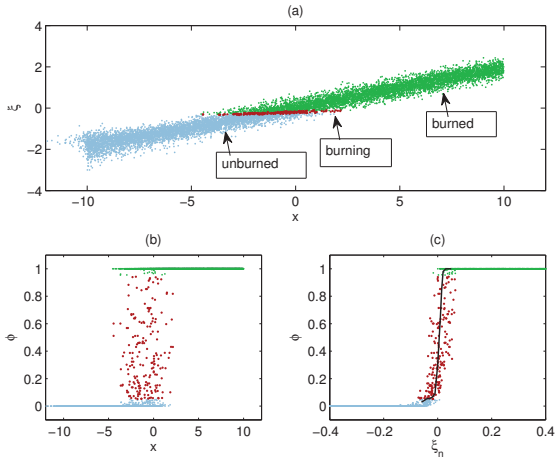

Figure 2: Simulation of a one-dimensional planar flame with 10000 particles and one-step chemistry: a) particle distributions in reference space versus physical space, b) particle progress variable in physical space and c) particle progress variable in reference space with the solid black line representing the flamelet solution (ξ-scale is magnified); light grey (blue) markers are unburned (ϕ <0.05), dark (red) markers are burning (0.05< ϕ <0.95) and light grey (green) markers are burned (ϕ >0.95).

Equation (6) is impractical for several reasons. Firstly, it is the consistency of the limiting parameters and not the scaling of the reference variable that is of primary importance. Secondly, the scaling of area A_ξ through the inertial interval remains unknown. Thirdly, only parameters in the vicinity of the flame affect the flame and, thus, are of interest. Hence, for our purposes, we apply constant scaling of ξ with two possible choices—

$$\text{inner scaling: } u = u_0,\ D = D_0,\ \xi = \xi_n \sim n \tag{7}$$

$$\text{outer scaling: } u = u_t,\ D = D_{\text{eff}},\ \xi = \xi_x \sim x. \tag{8}$$

Equation (7) interprets the reference variable ξ as representing the local distance n normal to the flame. Here, the propagation velocity corresponds to the laminar propagation speed u_0 and the diffusion coefficient in the ξ-space is the laminar diffusion coefficient D_0. In the outer scaling Eq. (8), the reference variable ξ is scaled in the same way as the global physical coordinate x and in this case the propagation speed in the reference space $u = u_t$ represents the turbulent propagation velocity. It is stressed that for outer scaling, the diffusion coefficient does not represent turbulent diffusivity D_t but an effective diffusivity specified by the equation

$$D_{\text{eff}} = D_0\lambda^2, \quad \lambda \equiv \frac{u_t}{u_0}, \tag{9}$$

found by rescaling the reference variable $\xi_x = \lambda\xi_n$.

These scaling equations represent alternative interpretations but not alternative models — these models are equivalent and can be obtained from each other by replacing the reference variable $\xi_x = \lambda\xi_n$. When interpreting the flame structure in the vicinity of the flame, the inner scaling must always be used irrespective of the actual scaling used in simulations. This is illustrated by a stochastic simulation of a one-dimensional planar flame using 10000 particles in Fig. 2, in which incoming velocity is selected to keep the flame steady near $x = 0$. Figure 2a shows topological similarity between the ξ and x with a thin reacting zone represented by dark markers. The normalized temperature or progress variable $\phi = (Y - Y_u)/(Y_b - Y_u)$ of particles is plotted in physical space in Fig. 2b, where substantial scattering is observed. The subscripts u and b are for unburned and burned particles respectively. In Fig. 2c, ϕ is plotted against ξ which is scaled as the local normal to the flame, revealing the thin flamelet structure located near $\xi_n = 0$. The scattering around the flamelet solution, which emulates the disturbance of the flame by turbulent fluid flow, is controlled by an MMC localness parameter. This indicates that, flamelet-consistent conditioning should involve a reference variable with a drift term reflecting the propagation of premixed flames. The same conclusion should apply to any model involving mapping-type closures with a smooth distribution (e.g. Gaussian). Although the level set variable is an intuitive choice for a reference variable, it is impractical due to the ambiguity of flame scaling in the inertial interval. A different approach to address the complexities of determining the flame position in multiple dimensions is considered next.

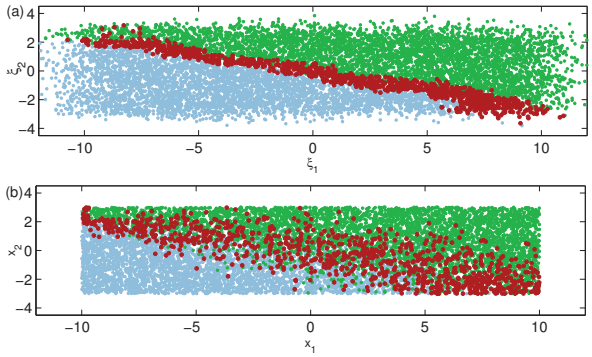

Figure 3: Simulation of a two-dimensional flame in a channel with one-step chemistry and 10000 particles: a) particle distributions in the reference space and b) particle distributions in physical space; legend per previous figure. The flame front is thin in the reference space and thicker in the physical space, with a clear correlation between the location of reacting particles in both spaces.

4. The reference variables represented by shadow positions.

The outer scaling with $\langle \xi^* | x \rangle = x$, is most convenient for specifying the position of the flame. Indeed, in this case the location of the flame in the reference space is interpreted as the average position of the flame in the physical space. If the problem is multi-dimensional, several reference variables $\langle \xi_i^* | \mathbf{x} \rangle = x_i$, with $i = 1, 2, 3$ must be prescribed. The system governing the evolution of the reference variables becomes

$$d\boldsymbol{\xi}^* = \mathbf{u}^* dt + \frac{\mathbf{x}^* - \boldsymbol{\xi}^*}{\tau_\xi} dt + (2D_{\text{eff}})^{1/2} d\omega_\xi^*, \tag{10}$$

which corresponds exactly to SPMM [36], a relatively new model suggested by Pope which is consistent with the principles of the MMC framework. The only difference is that D_{eff} is not linked to the turbulent diffusivity, but is selected to match the required u_t which can be estimated as $(2D_{\text{eff}}/\tau_c)^{1/2}$, where τ_c is the chemical timescale.

The drift velocity corresponds to the Lagrangian average physical velocity $\mathbf{u}^* = \mathbf{V}(\mathbf{x}^*, t)$ and $\mathbf{V} = \langle \mathbf{v} | \mathbf{x} \rangle$. If the flame position is fixed, one reference variable which is selected such that $\xi = \xi_f$ corresponds to the flame location is generally sufficient. However, the position and dynamics of the flame are unknown, practically. The shadow position model with an appropriately selected D_{eff} allows us to determine the position of the flame as part of the simulations. Equations (6) and (10) are similar but differ in two important respects. Firstly, model (10) is three-dimensional and spatially isotropic, allowing for arbitrary orientation of the flame, while it is attached to the surface $\xi = \xi_f$ in (6). Secondly, proper selection of D_{eff} allows Eq. (10) to match the inner and outer flame characteristics, while Eq. (6) endeavors to reproduce the whole scaling through the inertial interval.

Figure 3 illustrates the propagation of a turbulent premixed flame in a two-dimensional channel using one-step chemistry and 10000 particles. The flame is anchored at the top left corner by maintaining a perpetually burning particle there, while the slope is determined by the horizontal mean velocity and its turbulent propagation speed. A reflective boundary is imposed at the top and bottom of the channel. The vertical mean velocity in this case is zero. As expected, the flame is more localized in the space of the reference (shadow position) variables but dispersed in the physical space. The applied k-d-tree algorithm, which has been reliably used for mixing localization in non-premixed combustion [14], is fast but can produce odd mixing couples. Since premixed flames are more sensitive to localization than non-premixed cases, distance checks and post-selection of mixing couples are recommended. The k-d-tree localization is weighted by the characteristic values of ξ and x gradients, with emphasis on localization in the reference space.

The selection of an effective diffusion coefficient may also resemble the conventional modeling strategy of thickening the flame by artificially boosting molecular diffusion. The flexibility of different scalings is applied in MMC only to the reference variables but physical variables and parameters are not altered. Applying shadow positions as reference variables is effective for determining the flame position but requires localization of mixing in a six-dimensional space $(\mathbf{x}, \boldsymbol{\xi})$.

5. Second conditioning

The main purpose of using MMC in simulations of thin premixed flames is to prevent uncontrolled mixing across the flame. Characteristic scales along a flame are typically much larger than the flame thickness.

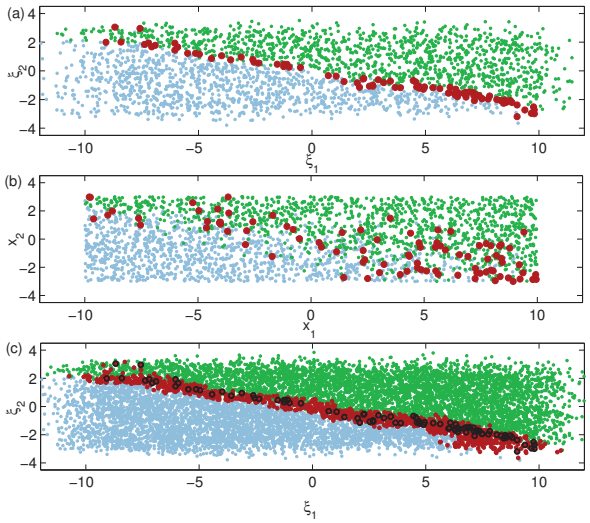

Figure 4: A simulation of a two-dimensional flame in a channel with one-step chemistry localized in ϕ°-space on reduced set of 2500 particles: particle distributions in (a) shadow-position reference space and (b) physical space; light grey (blue) markers—unburned (Y_2 <0.05), dark (red) markers—burning (0.05< Y_2 <0.95) and dark grey (green) markers—burned (Y_2 > 0.95); (c) reduced set of reacting particles is shown by the black circles in the foreground overlaid on the complete set of 10000 particles, with light grey (blue) markers—ϕ <0.05, dark (red) markers—0.05< ϕ <0.95 and dark grey (green) markers—ϕ > 0.95.

Hence, mixing along the flame can, in principle, occur between more distant particles without adversely affecting the quality of the simulations. If the position and direction of the flame is unknown *a priori*, three shadow position coordinates ξ_1, ξ_2 and ξ_3 can be used to account for any possible position and direction of the flame. This requires isotropic localization of mixing in $\xi-$space, necessitating a large number particles, which is computationally inefficient.

Conceptually, numerical efficiency can be improved in the context of MMC framework by tightening conditions for mixing across the flame and relaxing mixing along the flame. This can be done in many different ways, with second conditioning as one of the possibilities. The first conditioning is performed in the six-dimensional shadow position-physical coordinate space $(\boldsymbol{\xi}, \mathbf{x})$ for one-step chemical kinetics, as previously discussed. The progress variable ϕ is subsequently used (or ϕ°, after the modifications discussed below) for a second conditioning of multiple species describing realistic kinetics. Second conditioning is performed in the space $(\phi^\circ, \mathbf{x})$ or in the space $(\phi^\circ, \boldsymbol{\xi}, \mathbf{x})$ with increased weighting for ϕ°. This reduces the mixing distance between particles normal to the flame front, allowing more optimal use of computational resources. A smaller fraction of the original particles needs to be used in the evaluation of realistic chemical kinetics. This second level of conditioning is novel and distinct from second order conditioning. It is also unlike double conditioning; the former occurs sequentially while the latter occurs in parallel.

Progress variable seems to be a logical choice for conditioning having been repeatedly discussed in CMC [8], although this is not necessarily restricted to ϕ. In principle, any variable showing the evolution across the flame front is suitable for second conditioning. The nature of PDF simulations, however, demands some modifications of this variable. The first modification is to ensure that evolution of ϕ° is continuous. In general this may not be the case since, for example, conventional Curl's mixing can produce jumps. Deploying jump-free versions of mixing or spreading the jump over time step(s) are possible strategies to address this issue. The second modification is to permit the growth of ϕ° with time above $\phi = 1$ in the burned region. These changes may be needed for proper evaluation of slow reactions such as incomplete CO oxidation or for stabilising the flame localization. The main modification is that diffusion in the ϕ-space must exist for the flame can propagate against the incoming velocity of fluid. As in CMC with progress variable conditioning [8], the magnitude of this diffusion is determined by scalar dissipation N_ϕ of the progress variable. Since we intend to preserve the positive nature of the second reference variable, the expression $\phi^\circ = \phi \exp(\beta\omega_{\mathrm{OU}})$ is applied to introduce some mixing into the second reference space (i.e. progress variable space) and to stimulate the mixing of different particles. A standard bounded random Ornstein–Uhlenbeck process, ω_{OU} is applied to preserve the correlation of variables. The coefficient β is selected to match the expected overall level of diffusion in the second reference space.

Figure 4 illustrates the outcome of simulations with 2500 particles for the second level of conditioning instead of 10000, as used in Fig. 3. Both the scalars ϕ and Y_2 (which is normalized in the same way as the reaction progress variable ϕ) are subject to a one-step reaction with the same characteristic chemical time,

but are mixed differently. The progress variable ϕ is mixed with strong localization in the multi-dimensional space of the primary reference variables $\boldsymbol{\xi}$ (and a weaker localization in the physical space $\mathbf{x}$). The reactive variable Y_2 is mixed with strong localization in the secondary reference space ϕ° (with weaker localizations in $\boldsymbol{\xi}$- and $\mathbf{x}$-spaces). Hence, ϕ and Y_2 are mixed differently.

A comparison of the flame location in Fig. 3a (based on ϕ) and Fig. 4a (based on Y_2) using a fraction of the original particles show that both scalars occupy similar locations in the primary reference space. This comparison can be directly seen in Fig. 4c which overlays the burning Y_2 particles onto the full set of ϕ particles. The flame structure in physical space is also similar between Figs. 3b and 4b. It is possible to preserve a thin flame front with fewer reacting particles with second conditioning for a decrease in computational cost.

6. Conclusions

This work examines the extension of MMC to thin turbulent premixed flames, focusing on the selection of appropriate reference variables, with a general analysis suitable for different geometries and kinetic mechanisms. The results are illustrated by simulations with one-step kinetic mechanism and a high Zeldovich number. The main goal of using MMC in the context of Lagrangian PDF simulations is to make simulations consistent with the laminar flamelet structure. Essentially, MMC prevents the direct mixing of unburned and burned fluid, which is unphysical as it effectively bypasses location of the flame. Simultaneously, MMC does not compromise or alter the representation of mixing and reactions but functions only through conditioning the mixing operator by localizing it in a reference space.

From a physical perspective, using the level set variable is transparent, as the distance to the instantaneous position of the flame is more important for physical characteristics of the flow than absolute physical location. While choosing a reference variable based on the level set serves as a physical interpretation of the method, it is unsuitable for practical simulations given limited knowledge of premixed flame scaling through the inertial interval.

For more practical cases requiring a flexible method that allows for the determination of flame location, shadow positions are the best choice for the reference variables. The only difference between the reference variables discussed here to those in the non-premixed SPMM model is the replacement of the turbulent diffusion coefficient by an effective diffusion coefficient, which found from the turbulent flame propagation speed. The flexibility and geometric universality of this approach is, however, associated with additional computational expenses due to the need of localizing mixing in spaces of large dimensions.

The choice of a progress variable (with necessary modifications) as another MMC reference variable offers additional advantages. This approach, however, requires modeling the flame location by some alternative means and subsequently enforcing this location on PDF simulations. The competing requirements of universality and efficiency can be addressed with the use of second conditioning. Initial conditioning is performed by MMC modeling of the reaction progress variable using simple kinetics and shadow position reference variables. The progress variable can then be used for the second conditioning in MMC simulations with realistic kinetics.

We also note that knowledge of premixed combustion remains relatively limited and that further experimental and DNS investigations are required in order to deploy more efficient and accurate models for practical evaluation of realistic flames. MMC provides a good framework for such implementations.

Acknowledgements
This work is supported by the Australian Research Council under grant number DP120102294.

Appendix I: Propagation speed of flamelets

The MMC models considered here require the specification of a turbulent propagation velocity. Uncertainty remains for this key parameter, while scaling characteristics of premixed flames through the inertial interval are even less known. In the absence of rigorous formulae representing turbulent propagation speed u_t, we deploy relatively simple estimates that result in the so-called 4/7 power law [37], which produces a good match for the well-known parametrization of premixed propagation speeds by Bradley et al. [38]. These estimates are based on the cascade hypothesis [39, 40, 37] and are otherwise unrelated to theoretical basis of MMC, which can work with any other approximation for u_t. The 4/7 law is based on two major assumptions: i) that the scaling of premixed flame through inertial interval is consistent with Kolomogov scaling and ii) that this scaling needs modification to account for flame-generated turbulence.

According to conventional parametrizations [38], u_t depends on u_0, the turbulent integral length scale ℓ_t, the turbulent integral scale for velocity fluctuations v_t and the turbulent Reynolds number $\mathrm{Re} = v_t\ell_t/\nu$,

with viscosity as ν. Laminar flame thickness is estimated by $\ell_f = \nu/u_0$. In the vein of many theories, it is also assumed that the velocity fluctuations and u_t have the same scaling within the inertial interval, resulting in

$$\frac{u_t}{v_t} \approx \frac{u_0}{v_k}, \tag{11}$$

where v_k is the Kolmogorov velocity scale, which is estimated as $v_k \approx (\nu\varepsilon)^{1/4} \approx \nu(v_t^3/\ell_t)^{1/4}$ with the rate of dissipation given by $\varepsilon \approx v_t^3/\ell_t$. Equation (11), however, is inaccurate and needs to be modified to account for flame-generated turbulence.

At the largest scales, the flame propagates due to intrinsic turbulence of the flow field. The flame, however, produces additional fluctuations that cascade from the largest to smallest scales and alter the Kolmogorov scales. Towards the smallest scales, the flame propagates due to both the intrinsic turbulence and the turbulence generated at the largest scales. Assuming that ℓ_t and ν remain unchanged, and that the generated turbulent fluctuations v_t' are proportional to the turbulent flame speed ($v_t' \sim u_t$), we note that $v_k \sim v_t^{3/4}$ (so that $v_k' \sim v_t'^{3/4}$) and obtain

$$\frac{v_k'}{v_k} \approx \left(\frac{v_t'}{v_t}\right)^{3/4} \approx \left(\frac{u_t}{v_t}\right)^{3/4}, \tag{12}$$

where v_k' is new value of the Kolmogorov velocity scale that takes into account flame-generated turbulence v_t'. Since the flame propagates in intrinsic turbulence at large scales and in cascaded flame-generated turbulence at small scales, Eq. (11) needs to be modified to $u_t/v_t \approx u_0/v_k'$ to account for change in the Kolmogorov velocity scale. Then substituting of Eq. (12) into this relation yields

$$\frac{u_t}{v_t} \approx \frac{u_0}{v_k'} \approx \frac{u_0}{v_k}\frac{v_k}{v_k'} \approx \frac{u_0}{u_k}\left(\frac{u_t}{v_t}\right)^{-3/4}. \tag{13}$$

Solving this equation for u_t results in the formula,

$$\frac{u_t}{v_t} \approx 1.3\left(\frac{u_0}{u_k}\right)^{4/7}, \tag{14}$$

which is called the 4/7 power law with an empirical constant of 1.3 to match the BLL experimental data. This law [37] is agreement with parametrization of experimental data [38] as shown in Fig. 5, although the approximation becomes inaccurate when Ka > 1. With $u_t \approx (2D_{\text{eff}}/\tau_c)^{1/2}$,

$$\frac{u_t}{v_t} \approx \left(2\frac{D_{\text{eff}}}{\tau_c v_t^2}\right)^{1/2} \approx \left(2\frac{D_{\text{eff}}}{D_t}\frac{\tau_t}{\tau_c}\right)^{1/2} \approx \left(2\frac{D_{\text{eff}}}{D_t}\,\text{Da}\right)^{1/2}, \tag{15}$$

where $\tau_t = \ell_t/v_t$ is the macro timescale, $D_t \sim \ell_t v_t$ is the turbulent diffusion coefficient and Da is the Damköhler number. Comparing this equation with Eq. (14) results in

$$\frac{D_{\text{eff}}}{D_t} \approx \frac{0.39}{\text{Da}\,\text{Ka}^{4/7}} \sim \frac{\text{Ka}^{3/14}}{\text{Re}^{1/2}} \tag{16}$$

where the Karlovitz number defined by Bradley et al. [38] as

$$\text{Ka} = 0.157(v_t/u_0)^2\,\text{Re}_t^{-1/2} \tag{17}$$

is used so that the 4/7 law can be rewritten as

$$u_t \approx 1.3 v_t\left(\frac{0.508}{\text{Ka}^{1/2}}\right)^{4/7}. \tag{18}$$

If the Kolmogorov scaling (Eq. (11)) is used without accounting for flame-generated turbulence (which does not match experimental data well), then $D_{\text{eff}}/D_t \sim \text{Re}^{-1/2}$. In any case, the effective diffusion coefficient D_{eff} is significantly smaller than the turbulent diffusion coefficient D_t.

Appendix II: Numerical details

The model is implemented in a Monte-Carlo scheme where the PDF is represented by 10000 particles which are uniformly distributed in the physical space and initialized similarly in the shadow position space,

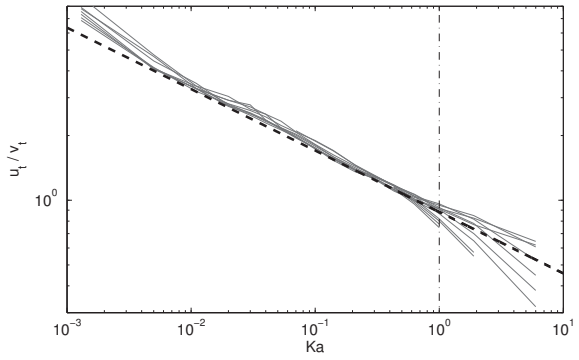

Figure 5: A comparison of the 4/7 power law (black dashed line) with the the Bradley-Lau-Lawes experimental data [38] (grey lines) with the flamesheet regime occurring to the left of the vertical dotted-dashed line where Ka <1.

when it is used as the reference variable. At each time step, particle properties are altered due to reaction, mixing and throughflow. Unity Lewis and Schmidt numbers are assumed, along with constant density. Length scales are ℓ_t and timescales are normalized by τ_t. With this normalization, $\ell_t = 1$, the velocity timescale $v_t = 1$ and τ_t of 1. The parameters described here are the same for all presented cases. Fluid viscosity $\nu = D = 0.001$, giving a turbulent Reynolds number $\mathrm{Re} = \ell_t v_t/\nu = 1000$.

Reactive scalars and progress variable evolve by a one-step irreversible reaction, in which the Arrhenius coefficient and the Zeldovich parameter are set to $A = 4000$ and $Z = 20$ respectively to give the characteristic chemical timescale τ_c of 0.1. The chemical timescale is found via asymptotic analysis of the reaction rate, $W(\phi) = A(1-\phi)e^{Z(\phi-1)}$, such that $\tau_c \approx Z^2/A$ in the limit of a large Zeldovich number. The Damköhler number $\mathrm{Da} = \tau_t/\tau_c$ is therefore 10. Laminar flame speed is estimated by $u_0 \approx (2D_0/\tau_c)^{1/2}$ where D_0 is the molecular diffusivity in physical space. Note that unlike localisation in physical space [21], which results in diffusion asymptotics only for low Da, the present localisation in the reference space is diffusion-driven for high Da. With D_0 set to 0.001, $u_0 \sim 0.14$, $\mathrm{Ka} \sim 0.25$ from Eq. (17), u_t is evaluated according to Eq. (18) and is used to set D_{eff}.

The progress variable also changes due to micromixing associated with a prescribed mixing timescale τ_m which controls MMC localization. Here, particles are mixed by a Modified Curl's mixing model [29] to a random extent. The particle pairing itself is not random, but controlled and localized based on assigned weightings to the reference variables. Particles are paired using a k-d tree algorithm and mixed. While the k-d tree is efficient, premixed flamelets are especially sensitive to the occasional pairing of distant particles, in contrast with the sensitivity observed in non-premixed simulations. *A priori* investigations of mixing distances are performed and, at this stage, it is found that mixing the closest 80% of particles satisfactorily reduces the incidence of remote particles mixing; caution is required in the selection of this percentage. The weightings for mixing are selected according to the expected gradients in the $\boldsymbol{\xi}$-$\mathbf{x}$-spaces.

References

[1] P. Libby, F. Williams (Eds.), Turbulent reacting flows, Springer-Verlag, Berlin, 1980.
[2] V. R. Kuznetsov, V. A. Sabelnikov, Turbulence and Combustion, Hemisphere Publishing Company, New York, USA, 1990.
[3] N. Peters, Turbulent combustion, Cambridge University Press, Cambridge, UK, 2000.
[4] R. O. Fox, Computational models for turbulent reacting flows, Cambridge University Press, Cambridge, UK, 2003.
[5] T. Poinsot, D. Veynante, Theoretical and numerical combustion, R. T. Edwards, Philadelphia, PA, 2005.
[6] R. S. Cant, E. Mastorakos, An introduction to turbulent reacting flows, Imperial College Press, London, UK, 2008.
[7] R. W. Bilger, Turbulent flows with nonpremixed reactants., in: P. Libby, F. Williams (Eds.), Turbulent Reacting Flows., Springer, 1980, Ch. 3, pp. 65–113.
[8] A. Y. Klimenko, R. W. Bilger, Prog. Energy Combust. Sci. 25 (6) (1999) 595–687.
[9] S. Pope, Prog. Energy Combust. Sci. 11 (1985) 119–192.
[10] D. C. Haworth, Prog. Energy Combust. Sci. 36 (2010) 168–259.
[11] A. Y. Klimenko, S. B. Pope, Phys. Fluids 15 (2003) 1907–1925.
[12] M. J. Cleary, A. Y. Klimenko, in Turbulent Combustion Modelling Advances, New Trends and Perspectives (eds. T. Echekki and E. Mastorakos), Springer, New York, 2011.
[13] M. J. Cleary, A. Kronenburg, Combust. Flame 151 (2007) 623–638.
[14] Y. Ge, M. J. Cleary, A. Y. Klimenko, Proc. Combust. Inst. 34 (2013) 1325–1332.
[15] S. B. Pope, Proc. Combust. Inst. 34 (2013) 1–34.
[16] S. Pope, M. Anand, Proc. Combust. Inst. 20 (1984) 403–410.
[17] M. S. Anand, S. B. Pope, Combust. Flame 67 (1987) 127–142.
[18] S. Pope, Ann. Rev. Fluid Mech. 19 (1987) 237–270.
[19] T. Hulek, R. P. Lindstedt, Combust. Flame 104 (1996) 481–504.

[20] D. C. Haworth, in: Proc. 2000 Summer Prog. CTR, Stanford University & NASA Ames, 2000.
[21] A. Y. Klimenko, S. B. Pope, Combust. Theory Mod. 16 (2012) 679–714.
[22] B. Sundaram, A. Klimenko, M. Cleary, Y. Ge, Combust. Theory Mod. (2016) 10.1080/13647830.2016.1174308.
[23] B. Sundaram, A. Y. Klimenko, M. J. Cleary, U. Maas, Proc. Combust. Inst. 35 (2015) 1517–1525.
[24] H. Chen, S. Chen, R. H. Kraichnan, Phys. Rev. Lett. 63 (1989) 2657–2660.
[25] S. B. Pope, Theoret. Comp. Fluid Dyn. 2 (1991) 255–270.
[26] L. Dialameh, M. J. Cleary, A. Y. Klimenko, Phys. Fluids 26 (2014) 025107.
[27] A. Wandel, R. P. Lindstedt, Proc. Combust. Inst. 34 (2013) 1365–1372.
[28] R. L. Curl, Aiche Journal 9 (1963) 175–181.
[29] J. Janicka, W. Kolbe, W. Kollman, Jrnl. Non-Equilib. Thermodyn. 4 (1977) 47–66.
[30] C. Dopazo, Phys. Fluids 18 (1975) 397410.
[31] A. Y. Klimenko, Combust. Flame 143 (2005) 369–385.
[32] A. Klimenko, D. Saulov, P. Massarotto, V. Rudolph, Transp. Porous Med. 92 (2012) 745–765.
[33] H. Pitsch, L. D. de Lageneste, Proc. Combust. Inst. 29 (2002) 2001–2008.
[34] A. G. Class, B. J. Matkowsky, A. Y. Klimenko, Jrnl. Fluid Mech. 491 (2003) 11–49.
[35] R. W. Bilger, Note in M. Namazian and L. Talbot and F.R. Robben, Proc. Combust. Inst. 20 (1984) 418.
[36] S. B. Pope, Phys. Fluids 25 (2013) 110803. doi:10.1063/1.4818981.
[37] A. Y. Klimenko, Combust. Sci. Tech. 139 (1998) 15–40.
[38] D. Bradley, A. K. C. Lau, M. Lawes, Phil. Trans. A Royal Soc. 338 (1992) 359387.
[39] V. Yakhot, Combust. Sci. Tech. 60 (1988) 191–214.
[40] G. I. Sivashinsky, Combust. Sci. Tech. 62 (1988) 77–96.